The Journal of Chemical Physics

RESEARCH ARTICLE | AUGUST 24 2020

The ozone–water complex: CCSD(T)/CBS structures and anharmonic vibrational spectroscopy of $O_3(H_2O)_n$, (n = 1 − 2)

Wallace C. H. Hui; Kono H. Lemke

J. Chem. Phys. 153, 084302 (2020)
https://doi.org/10.1063/5.0015597

The Journal of Chemical Physics ARTICLE scitation.org/journal/jcp

The ozone–water complex: CCSD(T)/CBS structures and anharmonic vibrational spectroscopy of $O_3(H_2O)_n$, (n = 1 – 2)

Cite as: J. Chem. Phys. 153, 084302 (2020); doi: 10.1063/5.0015597
Submitted: 1 June 2020 • Accepted: 4 August 2020 •
Published Online: 24 August 2020

Wallace C. H. Hui and Kono H. Lemke[a]

AFFILIATIONS

Department of Earth Sciences, University of Hong Kong, Pokfulam Road, Pok Fu Lam, Hong Kong, SAR

[a]Author to whom correspondence should be addressed: kono@hku.hk. Tel.: +852-2241-5474. Fax: +852-2517-6912

ABSTRACT

Ozone–water complexes $O_3(H_2O)_n$ (n = 1–2) have been studied using coupled cluster theory with triple excitations CCSD(T) with correlation consistent basis sets aug-cc-pVnZ (n = D, T, Q) and complete basis set (CBS) extrapolation techniques. We identified seven dimer (n = 1) and nine trimer species (n = 2) with open C_{2v} and cyclic D_{3h} ozone. Calculations at the CCSD(T)/CBS level of theory for C_{2v} $O_3(H_2O)$ on the counterpoise (CP)-corrected potential energy surface yield a dissociation energy of D_e = 2.31 kcal/mol and an O_3 central-oxygen (O_c) H_2O oxygen (O_w) distance $r[O_c\cdots O_w]$ of 3.097 Å, which is in good agreement with an experimental value of 2.957 Å [J. Z. Gillies *et al.*, J. Mol. Spectrosc. **146**, 493 (1991)]. Combining our CCSD(T)/CBS value of D_e for C_{2v} $O_3(H_2O)$ with our best estimate anharmonic CCSD(T)/aVTZ ΔZPE yields a D_o value of 1.82 kcal/mol; the CCSD(T)/CBS value of D_e for D_{3h} $O_3(H_2O)$ is 1.51 kcal/mol and yields an anharmonic CCSD(T)/aVTZ D_o = 0.99 kcal/mol. CCSD(T)/aVTZ dissociation energies and structures for C_{2v} $O_3(H_2O)_2$ are D_e = 4.15 kcal/mol, (D_o = 3.08 kcal/mol) and $r[O_c\cdots O_w]$ = 2.973 Å, and D_e = 2.64 kcal/mol (D_o = 1.68 kcal/mol) with $r[O_c\cdots O_w]$ = 2.828 Å for D_{3h} $O_3(H_2O)_2$. The results from *ab initio* molecular dynamics simulations, which consider dynamic and thermal effects in $O_3(H_2O)$, show that the $O_3(H_2O)$ complex remains stable at 50 K and dynamically interconverts between two hydrogen-bonded conformers with short $O_c\cdots O_w$ contacts (3.85 Å). Carr–Parrinello molecular dynamic (CPMD) simulations for $O_3(H_2O)$ and $O_3(H_2O)_2$ at 100 K demonstrate that $O_3(H_2O)_2$ remains structurally intact, whereas $O_3(H_2O)$ dissociates to free ozone and water, a feature consistent with the larger average binding energy in $O_3(H_2O)_2$ (2.2 kcal/mol) vs that in $O_3(H_2O)$ (1.8 kcal/mol). Finally, the results from CCSD(T)/CBS and CPMD simulations demonstrate that the large inter-trimer binding energies in $O_3(H_2O)_2$ would give rise to an elevated trimer/dimer population ratio, making $O_3(H_2O)_2$ a particularly stable and spectroscopically detectable complex.

I. INTRODUCTION

The $O_3(H_2O)$ dimer has attracted considerable attention as an atmospherically and environmentally important complex, and its presence in the upper atmosphere is directly related to the photostability of O_3.[1] For example, the $O_3(H_2O)$ complex has been implicated as a precursor participating in the photolytic generation of hydroxyl radicals in the Earth's atmosphere,[2–5] which is an important oxidant involved in the destruction of atmospheric pollutants such as CO.[6] Interactions between ozone and water molecules are also considered important due to the potential existence of hydrated complexes in exoplanet atmospheres with photosynthetic O_3 input.[7]

The principal source of O_3 in the Earth's stratosphere stems from photolytic ozone–oxygen cycling, in which O atoms recombine with O_2 to form O_3. The major source of tropospheric ozone, on the other hand, stems from the combustion of fossil fuels, with the most important precursor compounds being molecular hydrocarbons and nitrogen oxides.[8]

Unlike atmospheric O_2 and N_2, ozone in the presence of H_2O would exist as $O_3(H_2O)_n$ with varying numbers of hydrating water molecules due to the relatively large dissociation energy of $O_3(H_2O)$ (D_o = 1.27 kcal/mol);[9] the dissociation energy for $O_3(H_2O)$, however, is only ~40% of the value reported for $(H_2O)_2$ (D_o = 3.2 kcal/mol),[10] but nevertheless larger, by

around 1 kcal/mol than the best estimate coupled cluster/complete basis set [CCSD(T)/(CBS)] dissociation energies for $O_2(H_2O)$ (D_o = 0.17 kcal/mol)[11] and $N_2(H_2O)$ (D_o = 0.41 kcal/mol).[12] The main reason for these large differences in dissociation energies, in particular, between $O_3(H_2O)$, $N_2(H_2O)$, and $O_2(H_2O)$, is rooted in the high polarizibility of ozone (3.079 Å^3)[13] and the accompanying charge rearrangement upon solvation by water. Both N_2 and O_2, on the other hand, have relatively low polarizibilities, at 1.710 Å^3 and 1.560 Å^3,[14] respectively, and thus, no significant charge redistribution occurs once these molecules are bound to water. Thus, there is a critical need for accurate structure and energetic data for ozone–water complexes such as $O_3(H_2O)_n$, using high level theoretical calculations.

The $O_3(H_2O)$ complex has been studied in detail using structure-sensitive infrared (IR)[15–19] and microwave spectroscopy,[20] as well as theoretical methods, including density functional theory (DFT),[21] Møller–Plesset perturbation theory (MPn),[20,22–25] CCSD(T),[9,18,26] and complete active space self-consistent field (CASSCF)[27] calculations. The reported CCSD(T)/CBS dissociation energy D_e for $O_3(H_2O)$ is 2.40 kcal/mol, and the harmonic D_o value is 1.27 kcal/mol.[9,26] To the best of our knowledge, there are no experimental determinations of the dissociation energy for $O_3(H_2O)$. The structure of the $O_3(H_2O)$ complex was first probed using microwave spectroscopy, providing an intermolecular distance $r[O_c\cdots O_w]$ of 2.96 Å.[20] In the case of the trimer complex $O_3(H_2O)_2$, the dissociation energy D_e for the reaction $O_3(H_2O)_2 = O_3 + (H_2O)_2$ is 4.61 kcal/mol at the CCSD(T)/CBS level of theory.[9]

In this study, we present theoretical results for the dimer $O_3(H_2O)$ and trimer $O_3(H_2O)_2$, with open (C_{2v}) and cyclic (D_{3h}) forms of ozone, and these results have been obtained at the CCSD(T) level of theory with Dunning's augmented correlation consistent basis sets aug-cc-pVnZ (n = D, T, Q) basis sets up to the CBS limit. We also report the results for the CCSD(T) dissociation energies D_o with anharmonic zero-point energy (ZPE_F) corrections. The main goal of this work is to (i) calculate accurate structures and energies of $O_3(H_2O)_n$ for n = 1–2, (ii) report anharmonic CCSD(T) vibrational frequencies and values of D_o, and (iii) using Carr–Parrinello molecular dynamic (CPMD) simulations to predict the solvation behavior of $O_3(H_2O)$ and $O_3(H_2O)_2$ at 50 K, 100 K, and 150 K.

II. COMPUTATIONAL METHODS

The structures of O_3, H_2O, $O_3(H_2O)$, and $O_3(H_2O)_2$ have been optimized with coupled cluster CCSD(T) theory in combination with correlation consistent series basis sets aug-cc-pVnZ with n = D, T, Q (abbreviated as aVDZ, aVTZ, and aVQZ, respectively)[28] that permit extrapolation of energetic and spectroscopic properties to the full CBS limit. Equilibrium structures of $O_3(H_2O)$ and $O_3(H_2O)_2$ were first optimized at the CCSD(T)/aVDZ level of theory, followed by CCSD(T)/aVTZ optimizations and CCSD(T)/aVQZ single point energy (SPC) calculations. Harmonic frequencies were obtained at the CCSD(T) level of theory, with aVDZ and aVTZ basis sets for $O_3(H_2O)$ and aVDZ for $O_3(H_2O)_2$, and these frequencies were scaled using standard scaling factors [$\lambda_{CCSD(T)/aVDZ}$ = 0.971, $\lambda_{CCSD(T)/aVTZ}$ = 0.964, and $\lambda_{CCSD(T)/aVQZ}$ = 0.958]. Anharmonic frequencies were computed using vibrational second-order perturbation theory (VPT2) at the CCSD(T)/aVDZ level for the water and ozone monomers, $O_3(H_2O)$, and $O_3(H_2O)_2$; CCSD(T)/aVTZ anharmonic vibrational frequencies for $O_3(H_2O)$ were obtained using a scheme in which anharmonic corrections are retrieved at a lower level of theory, i.e., CCSD/aVDZ. The approach used to obtain anharmonic corrections to vibrational frequencies is written as follows:

$$\nu_i[\mathrm{CCSD(T)/aVTZ}] = \omega_i[\mathrm{CCSD(T)/aVTZ}] + \{\nu_i[\mathrm{CCSD/aVDZ}] - \omega_i[\mathrm{CCSD/aVDZ}]\}, \quad (1)$$

where ω_i and ν_i are the harmonic and anharmonic vibrational frequencies in O_3, H_2O, $O_3(H_2O)$, and $O_3(H_2O)_2$, respectively. The approach adopted here, in particular, the use of the CCSD level of theory, was prompted by the need to capture both corrections at a computationally feasible level of theory, without the use of MP2 theory, given the latter's well-known deficiency in estimating the correct order of vibrational frequencies in ozone.[29,30] Anharmonic frequencies of cyclic $O_3(H_2O)$ and $O_3(H_2O)_2$ have been estimated by the following scheme:

$$\nu_i[\mathrm{CCSD(T)/aV}n\mathrm{Z}] = \omega_i[\mathrm{CCSD(T)/aV}n\mathrm{Z}] + \{\nu_i[\mathrm{MP2/aV}n\mathrm{Z}] - \omega_i[\mathrm{MP2/aV}n\mathrm{Z}]\}, \quad (2)$$

with n = T for $O_3(H_2O)$ and n = D for $O_3(H_2O)_2$.

The CBS extrapolation formula employed in this study is a three-point CBS extrapolation scheme[31] and is written as

$$\mathrm{E}(n) = \mathrm{E}(\infty) + \mathrm{B}e^{-(n-1)} + \mathrm{C}e^{-(n-1)^2}, \quad (3)$$

where n represents the cardinal number for the respective basis sets (aVDZ: 2, aVTZ: 3, and aVQZ: 4). E(n) is the parameter of interest at the respective aVnZ basis set, and E(∞) is the CBS limit parameter; B and C are constants obtained by least-square fitting the respective aVDZ, aVTZ, and aVQZ values to Eq. (3). We also employed a two-point CBS extrapolation scheme[32] according to

$$\mathrm{E}(n) = \mathrm{E}(\infty) + \mathrm{A}/n^3, \quad (4)$$

where n is the cardinal number of the basis set (aVTZ: 3 and aVQZ: 4) and A is a constant obtained by fitting a sequence of two correlation consistent basis sets to Eq. (4). CBS values of D_e have been estimated by taking the differences between individual dimer and monomers energies E_h (see Table I). Harmonic and anharmonic zero-point energies and corresponding ZPE-corrected dissociation energies D_o were calculated from harmonic and anharmonic frequencies using the relationships,

$$\mathrm{ZPE}_H = 1/2 \sum_0^i \omega_i[\mathrm{CCSD(T)/aV}n\mathrm{Z}], \quad (5)$$

$$\mathrm{ZPE}_F = 1/2 \sum_0^i \nu_i[\mathrm{CCSD(T)/aV}n\mathrm{Z}], \quad (6)$$

$$D_o = D_e - [\mathrm{ZPE}_F(O_3 - H_2O) - \mathrm{ZPE}_F(H_2O) - \mathrm{ZPE}_F(O_3)], \quad (7)$$

TABLE I. Energies E_h (hartrees), structure parameters, and vibrational frequencies of O_3 (scaled-harmonic and anharmonic).

Method	Basis set	Energy (E_h)	r_{OO} (Å)	θ (deg)	ω_2 (cm^{-1})	ω_3 (cm^{-1})	ω_1 (cm^{-1})	ν_2 (cm^{-1})	ν_3 (cm^{-1})	ν_1 (cm^{-1})
				Open O_3 (C_{2v})						
MP2	aVDZ	−224.964 529	1.291	116.3	715	2206	1111	747	2205	1191
	aVTZ	−225.182 065	1.278	116.8	708	2099	1107	753	2154	1203
	aVQZ	−225.290 003	1.275	116.9	717	2097	1119	758	2145	1209
	CBS[D,T,Q]	−225.355 466	1.273	117.0	...	2099	...	761	2141	1213
	CBS[T,Q]	−225.368 769	1.273	117.0	724	2096	1128	762	2138	1213
CCSD	aVDZ	−224.937 949	1.258	117.3	731	1183	1212	741	1178	1223
	aVTZ	−225.148 179	1.244	117.8	730	1207	1223	756	1235	1263
	aVQZ	−225.251 740	1.241	117.9	743	1234	1245	765	1254	1277
	CBS[D,T,Q]	−225.314 495	1.239	118.0	...	...	...	771	1265	1285
	CBS[T,Q]	−225.327 312	1.239	118.0	...	...	...	772	1268	1287
CCSD(T)	aVDZ	−224.975 509	1.284	116.6	684	943	1083	685	888	1056
	aVTZ	−225.196 578	1.269	117.2	694	1025	1118	706	1004	1119
	aVQZ	−225.302 929	1.266	117.3	698	1042	1125	714	1059	1154
	CBS[D,T,Q]	−225.367 195	1.264	117.3	700	1051	1129	719	1092	1175
	CBS[T,Q]	−225.380 536	1.264	117.4	701	1054	1130	720	1099	1180
CCSD(T)[a]	cc-pVDZ	−224.941 382	1.287	116.8	703	976	1129	...	...	...
CCSD(T)[b]	cc-pVTZ	−225.165 815	1.275	116.9	717	1057	1152	699	975	1105
CCSDT[a]	cc-pVDZ	−224.941 197	1.286	116.7	705	1077	1141	...	...	...
MRCI[c]	cc-pVQZ	−225.142 160	1.272	116.8	719	1103	1141	...	...	...
icMRCI+Q[d]	aVQZ	...	1.274	116.9	719	1105	1125	699	1055	1101
Expt.			1.273[e]	116.8[e]				701[f]	1042[f]	1103[f]
				Cyclic O_3 (D_{3h})						
MP2	aVDZ	−224.900 783	1.479	60.0	754	...	954	782	...	976
	aVTZ	−225.122 416	1.451	60.0	777	...	1014	817	...	1053
	aVQZ	−225.230 246	1.447	60.0	786	...	1028	821	...	1061
	CBS[D,T,Q]	−225.295 493	1.445	60.0	791	...	1035	822	...	1064
	CBS[T,Q]	−225.308 933	1.444	60.0	793	...	1038	824	...	1067
CCSD	aVDZ	−224.894 561	1.444	60.0	788	...	1103	798	...	1118
	aVTZ	−225.109 710	1.419	60.0	820	...	1156	849	...	1196
	aVQZ	−225.213 232	1.415	60.0	835	...	1176		...	
	CBS[D,T,Q]	−225.275 789	1.413	60.0	...	...	...		...	
	CBS[T,Q]	−225.288 775	1.412	60.0	...	...	...		...	
CCSD(T)	aVDZ	−224.923 560	1.467	60.0	721	...	1012	727	...	1019
	aVTZ	−225.148 975	1.442	60.0	768	...	1082	781	...	1099
	aVQZ	−225.255 350	1.437	60.0	772	...	1085	790	...	1109
	CBS[D,T,Q]	−225.319 480	1.434	60.0	773	...	1085	794	...	1113
	CBS[T,Q]	−225.332 975	1.433	60.0	775	...	1087	797	...	1116
icMRCI+Q[g]	cc-pVQZ	...	1.442	60.0	...	...	...	783	...	1100
MRDCI[h]	aVQZ	...	1.448	60.0	...	...	...	791	...	1088
MRCISD+Q[i]	aVTZ	...	1.449	60.0	859	...	1209	...	...	...

[a]Reference 44.
[b]Reference 45.
[c]Reference 46.
[d]Reference 47.
[e]Reference 42.
[f]Reference 43.
[g]Reference 50.
[h]Reference 49.
[i]Reference 51.

where ZPE_H and ZPE_F are the harmonic and fundamental zero-point energies and D_e and D_o are the uncorrected and ZPE-corrected dissociation energies, respectively. All calculations were carried out with the CFOUR[33,34] and the Gaussian 09[35] software packages.

Molecular dynamics simulations were carried out based on the Carr–Parrinello molecular dynamics approach using the CPMD software.[36] CPMD production runs were undertaken following wavefunction optimization and trial thermal CPMD runs to estimate values for the fictitious kinetic energy and mass parameters. All production CPMD calculations were performed using the generalized-gradient approximation (GGA) Becke-Lee-Yang-Parr (BLYP) exchange–correlation functional[37,38] in combination with the Kleinman–Bylander pseudo potentials for O and H[39] and a plane-wave cutoff of 25 Ry. The CPMD simulation was set up to contain the C_{2v} $O_3(H_2O)$ and $O_3(H_2O)_2$ complexes in a periodically repeated cubic simulation cell with a size dimension $16 \times 16 \times 16$ Å^3 in order to ensure gas-phase-like conditions. Production CPMD simulations were undertaken at 50 K, 100 K, and 150 K for 30 ps at 4 a.u. (0.096 fs) time steps and a fictitious electron mass of 400 a.u. (3.65×10^{-28} kg). All CPMD simulations were performed in the canonical NVT ensemble employing the Nosé–Hoover thermostat. Representative geometries of $O_3(H_2O)$ and $O_3(H_2O)_2$ highlighting distinct stages in the solvation behavior of ozone were analyzed in order to better understand the time- and temperature-dependent solvation dynamics in both complexes.

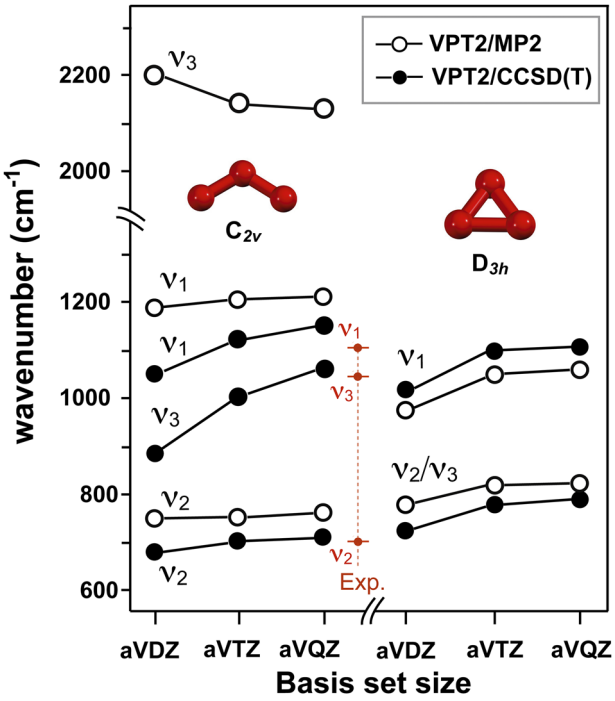

FIG. 1. Experimental and anharmonic CCSD(T) frequencies as a function of basis set for open (C_{2v}) and cyclic (D_{3h}) O_3.

III. RESULTS AND DISCUSSION

A. Monomers

The CCSD(T)/CBS level OH distance and bond angles in H_2O are 0.958 Å and 104.6°, respectively, and these are in good agreement with experimental values[40] of 0.957 Å and 104.5° (see Table 1S of the supplementary material). The results from anharmonic frequency calculations for H_2O show that the symmetric (ν_1) and asymmetric OH-stretching (ν_3) frequencies converge systematically to the CBS limit of ν_1 = 3665 and ν_3 = 3767 cm^{-1}, respectively, whereas those for the bending frequency ν_2 do not converge toward the CBS limit and instead yield a CCSD(T)/aVQZ value of ν_2 = 1601 cm^{-1}; the corresponding experimental values are ν_1 = 3657 cm^{-1}, ν_3 = 3756 cm^{-1}, and ν_2 = 1595 cm^{-1}.[41] Applying a two-point CBS extrapolation using the aVnZ (n = T, Q) basis set range yields ν_1 = 3667 cm^{-1}, ν_3 = 3769 cm^{-1}, and ν_2 = 1605 cm^{-1}, revealing no significant improvement over the results obtained from the three-point CBS extrapolation.

Energies, structure parameters, and anharmonic frequencies at the CCSD(T)/aVnZ level of theory for C_{2v} and D_{3h} O_3 are listed in Table I together with experimental[42,43] and reported multireference configuration interaction (MRCI) results.[46,47,50] The best estimate CCSD(T)/CBS O–O distance and angle in C_{2v} ozone is 1.264 Å and 117.3°, respectively, and these values are in excellent agreement with the experimental results. For example, the CCSD(T)/CBS O–O distance in C_{2v} ozone is shorter than experiment by just 0.009 Å, and the angle is larger by around 0.4° than the experimental value.[42] We also carried out a Mulliken population analysis of the charge distribution in C_{2v} O_3 at the CCSD(T)/aVTZ level of theory, and these results show that a positive charge (0.34e) is located on the central oxygen atom O_c, whereas both terminal oxygen sites O_t have smaller negative charges at −0.17e, which is consistent with previous charge estimates derived from CCSD/aVTZ calculations (O_c: 0.36e; O_t: −0.18e).[26]

Anharmonic CCSD(T)/aVnZ vibrational frequencies for the C_{2v} and D_{3h} forms of ozone are shown in Fig. 1, and these are given for the full basis set range aVnZ (n = D, T, Q) and CBS limit together with the results from MP2 calculations. As seen, symmetric (ν_1), asymmetric stretching (ν_3) and bending (ν_2) frequencies for C_{2v} O_3 converge smoothly to CBS limit values of 1175 cm^{-1}, 1092 cm^{-1}, and 719 cm^{-1}, with corresponding experimental values of ν_1, ν_3, and ν_2 at 1103 cm^{-1}, 1042 cm^{-1}, and 701 cm^{-1}, respectively.[43] The results from two-point CBS extrapolations using the aVnZ (n = T, Q) basis set sequence are also listed in Table I, and these are blue-shifted by ~3 cm^{-1} relative to results obtained from three-point CBS extrapolation calculations. Also shown in Table I are theoretical results from reported CCSD(T)[44,45] and MRCI calculations[46,47] using Dunning-style basis sets, and these are generally in good agreement with our CCSD(T) results. MP2 calculations with aVnZ (n = D, T, Q) basis sets, on the other hand, give rise to bending (ν_2) and stretching frequencies (ν_1, ν_3) that exhibit large deviations from experiment: for example, the MP2/CBS value of the asymmetric stretching frequency ν_3 is around 1200 cm^{-1} larger than the experimental value of 1042 cm^{-1} and 1050 cm^{-1} larger than our best CCSD(T)/CBS estimate (1092 cm^{-1}), which is due to the well-known deficiency of MP2 theory in describing the ionic and biradical character of ozone.[29,30,48]

CCSD(T) estimates for the O–O bond distance and angle in D_{3h} O_3 at the CBS limit are 1.433 Å and 60.0°, and these are in excellent agreement with the previous MRDCI/aVQZ calculations that yielded values of 1.448 Å and 60.0°, respectively.[49] There are, to our knowledge, no measured vibrational frequencies for the cyclic form of ozone, with the exception of two theoretical studies that predicted IR vibrational frequencies for O_3 using MRDCI[49] and icMRCI+Q[50] calculations. Table I presents energies and vibrational frequencies of cyclic O_3, and these have been calculated at the MP2/aV*n*Z and CCSD(T)/aV*n*Z level of theory and are compared against the results from reported MRCI calculations.[49–51] As seen from Table I, anharmonic MP2 and CCSD(T) frequencies for D_{3h} O_3 converge smoothly to their respective CBS[T, Q] limits (ν_2 = 797 cm^{-1} and ν_1 = 1116 cm^{-1}), with small (~3 cm^{-1}) differences between CBS extrapolations using [D, T, Q] and [T, Q] basis set sequences; it is also worth noting that these results agree relatively well with previously reported high-level MRDCI/aVQZ results[49] (ν_2 = 791 cm^{-1} and ν_1 = 1088 cm^{-1}), despite minor basis set differences. Figure 1 also summarizes the results from our anharmonic MP2 and CCSD(T) frequency calculations for D_{3h} O_3 and shows that the doubly degenerate bending mode ν_2 and symmetric stretching mode ν_1 smoothly converge toward MP2/CBS[T, Q] limit values of 824 cm^{-1} and 1067 cm^{-1}, and to 797 cm^{-1} and 1116 cm^{-1} with CCSD(T)/CBS[T, Q], respectively. An interesting feature of these results, however, is the large discrepancy between MP2 results for D_{3h} and C_{2v} O_3: for instance, vibrational frequencies of the bending ν_2 and stretching modes ν_1 in D_{3h} ozone are reasonably well-described at the MP2/aV*n*Z level of theory; however, the same method fails to reproduce the correct frequency positions and ordering in C_{2v} O_3. An explanation for this discrepancy is that MP2 frequency calculations, in particular, for the asymmetric stretch ν_3 in C_{2v} ozone, are hampered by the fact that the MP2 wavefunction does not accurately capture the dual ionic (82%) and biradical (18%) character of this molecule, which give rise to inaccurate frequency estimates, in particular, for the ν_3 mode.[52] Finally, if we apply our CCSD(T)/CBS energies for the D_{3h} and C_{2v} forms of O_3, we arrive at a ring opening energy of D_e = 29.9 kcal/mol, which is consistent with a previously reported UCCSD(T)/aVQZ value of 29.5 kcal/mol[51] and only slightly lower than the high-level MRCISD/aVQZ ring opening energy of 31.4 kcal/mol.[51]

B. C_{2v} $O_3(H_2O)$

The results from CCSD(T)/aV*n*Z (*n* = D, T) structure optimizations for four C_{2v} $O_3(H_2O)$ complexes are shown in Fig. 2, and these results are listed as a function of basis set size in Table II. For the global minimum $O_3(H_2O)$ isomer IA, the intermolecular distance $r[O_c\cdots O_w]$ between ozone and water is 3.165 Å and 3.097 Å at the CCSD(T)/aVDZ and CCSD(T)/aVTZ level of theory, respectively; the corresponding value of $r[O_t\cdots H_w]$ for isomer IA is 2.387 Å, and this value is in fair agreement with a reported QCISD/aVTZ level distance of 2.565 Å.[9] For structures IB, IC, and ID, the CCSD(T)/aVTZ values of $r[O_t\cdots H_w]$ are 2.221 Å, 2.123 Å, and 2.255 Å (see Fig. 2), and these results, in general, compare favorably with the previously reported QCISD/aVTZ distance values of 2.298 Å, 2.229 Å, and 2.316 Å, respectively.[9] In the case of $O_3(H_2O)$ isomer IA, we predict a small charge transfer from H_2O to O_3 (0.02*e*), resulting in an increase in the negative charge on the O_t site of ozone, and the positive charge at the O_c site is shifted from 0.34*e* to 0.37*e* (see Fig. 2). The charges on the ozone O_t and O_c sites in all four $O_3(H_2O)$ isomers (IA–ID) sum up to around −0.02*e* (IA) to −0.05*e* (ID), indicating that there is a moderate but consistent charge migration from H_2O to O_3 in all four complexes. The attachment of a water molecule onto ozone, as in the case of $O_3(H_2O)$ IA, gives rise to a noticeable charge increase at the O_t site (−0.17*e* to −0.20*e*) and a corresponding charge shift at the O_c site from 0.34*e* to 0.37*e*.

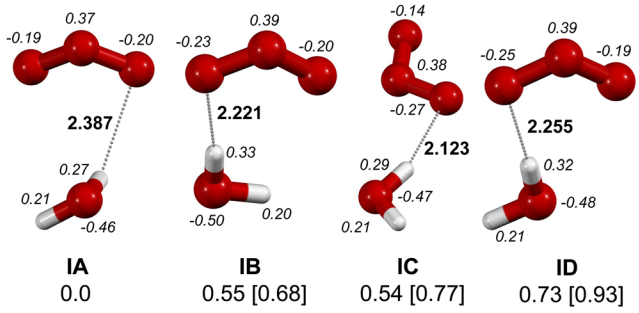

FIG. 2. CCSD(T)/aVTZ equilibrium structures (distances in Å), Mulliken charges (italicized), and CCSD(T)/CBS relative energies, without and with ZPE corrections (square brackets) in kcal/mol for C_{2v} $O_3(H_2O)$ complexes. IA: non-planar, IB–ID: planar.

Table II shows that the dimer energies E_h of all four C_{2v} $O_3(H_2O)$ complexes systematically converge to the CBS limit, with isomer IA found to be the most stable complex. At the CCSD(T)/aVDZ level of theory, the difference in energy between isomer IA and fourth-ranked complex ID is 0.22 kcal/mol; the second- and third-ranked $O_3(H_2O)$ structures are close to isoenergetic at 0.17 kcal/mol and 0.18 kcal/mol, relative to the global minimum isomer IA, respectively. Basis set expansion to aVTZ reduces the energy difference between structures IA and IB to 0.01 kcal/mol, while the ranking is reversed for IC and ID, and the gap between the global minimum and the lowest ranked isomer is reduced to 0.14 kcal/mol. In other words, the energetic spacing between $O_3(H_2O)$ isomers at the CCSD(T)/aVTZ level of theory is compacted with respect to the results from CCSD(T)/aVDZ calculations. Basis set expansion to aVQZ induces an energetic reordering: IA (0.0 kcal/mol), IB (0.3 kcal/mol), IC (0.4 kcal/mol), and ID (0.5 kcal/mol), and these results are consistent with those obtained from CCSD(T)/aVDZ calculations; Table II also presents CCSD(T)/CBS value of E_h from two- and three-point CBS extrapolations using Eqs. (3) and (4), and these rank isomers IA, IB, IC and ID at 0.0 kcal/mol, 0.5 kcal/mol, 0.5 kcal/mol, and 0.7 kcal/mol, respectively.

Figure 3 presents the CCSD(T)/aV*n*Z dissociation energies D_e as a function of basis set size up to the CBS limit using Eq. (4). For IA, the CP-uncorrected values of D_e are 2.94 (aVDZ), 2.97 (aVTZ), 2.57 (aVQZ), and 2.30 kcal/mol at the CCSD(T)/CBS limit (calculated employing CBS limit values of E_h), and the CP-corrected values of D_e for dimer IA are 1.72 (aVDZ), 2.12 (aVTZ), 2.24 (aVQZ), and 2.31 kcal/mol at the CBS limit (see Table II).The

TABLE II. CCSD(T)/aVnZ dissociation energies (D_e), scaled-harmonic dissociation energies (D_o), and structural parameters for C_{2v} $O_3(H_2O)$.

Isomer	Basis set	Energy (E_h)	D_e (kcal/mol)[a]	D_o (kcal/mol)[a]	$r[O_c\cdots O_w]$ (Å)
IA	aVDZ	−301.256 343	2.94 [1.72]	1.74 [0.52]	3.165
	aVTZ	−301.558 848	2.97 [2.12]	1.86 [1.00]	3.097
	aVQZ[b]	−301.702 257	2.57 [2.24]	...	...
	CBS[D,T,Q][c]	−301.788 762	2.30 [2.31]	...	...
	CBS[T,Q][d]	−301.806 907	2.28 [2.33]	...	...
IB	aVDZ	−301.256 075	2.77 [1.66]	1.68 [0.57]	3.812
	aVTZ	−301.558 828	2.96 [1.83]	1.71 [0.58]	3.792
	aVQZ[b]	−301.701 736	2.24 [1.93]	...	...
	CBS[D,T,Q][c]	−301.787 894	1.75 [1.99]	...	...
	CBS[T,Q][d]	−301.806 020	1.72 [2.01]	...	...
IC	aVDZ	−301.256 054	2.76 [1.66]	1.42 [0.32]	3.138
	aVTZ	−301.558 626	2.83 [1.78]	1.49 [0.44]	3.369
	aVQZ[b]	−301.701 658	2.19 [1.89]	...	...
	CBS[D,T,Q][c]	−301.787 906	1.76 [1.96]	...	...
	CBS[T,Q][d]	−301.806 033	1.73 [1.97]	...	...
ID	aVDZ	−301.255 993	2.72 [1.58]	1.58 [0.44]	3.744
	aVTZ	−301.558 714	2.89 [1.70]	1.58 [0.39]	3.732
	aVQZ[b]	−301.701 515	2.11 [1.80]	...	...
	CBS[D,T,Q][c]	−301.787 601	1.57 [1.86]	...	...
	CBS[T,Q][d]	−301.805 721	1.53 [1.87]	...	...
Expt.					2.957[e]

[a]CP-corrected D_e and D_o in square brackets.
[b]SPC on aVTZ geometry.
[c]Calculated by fitting E_h values to Eq. (3).
[d]Calculated by fitting E_h values to Eq. (4).
[e]Center of mass measurement from Ref. 20.

CCSD(T)/CBS limit values of D_e for the local minima IB, IC, and ID are 1.75 kcal/mol, 1.76 kcal/mol, and 1.57 kcal/mol, respectively, whereas CP-corrected dissociation energies are 1.99 kcal/mol, 1.96 kcal/mol, and 1.86 kcal/mol, respectively, and thus, CP-corrected and uncorrected CCSD(T)/CBS values of D_e differ by no more than 0.2 kcal/mol. Inspection of our CP-uncorrected dissociation energies D_e in Fig. 3 also shows that these display non-convergence behavior with respect to the basis set size, a feature reported previously for the dissociation energies of $(HF)_2$[53,54] and $(H_2S)_2$.[55] The CCSD(T)/CBS limit value of D_e for IA is around 0.1 kcal/mol lower than reported CBS dissociation energy values,[9,26] which is somewhat surprising given that reported CCSD and QCISD equilibrium structures were used together with CCSD(T) single point calculations to estimate D_e at the CBS limit. Finally, it is worth noting that the value of D_e for $O_3(H_2O)$ isomer IA is relatively small compared against other hydrogen- and dispersion-bound ozone complexes: specifically, our CCSD(T)/CBS value of D_e for $O_3(H_2O)$ (2.31 kcal/mol) represents just 45% of the water dimer CCSD(T)/CBS dissociation energy (D_e = 5.1 kcal/mol)[56] and is only moderately larger than the CCSD(T)/CBS dissociation energy for the ozone dimer $(O_3)_2$ (D_e = 2.2 kcal/mol).[57]

Table II lists ZPE-corrected dissociation energies D_o at the CCSD(T)/aV*n*Z (*n* = D, T) using scaled-harmonic vibrational frequencies. The CP-corrected CCSD(T)/aVTZ value of D_o for IA is 1.00 kcal/mol, and CP-corrected values of D_o for isomer IB, IC, and ID are 0.58 kcal/mol, 0.44 kcal/mol, and 0.39 kcal/mol respectively. It is worth mentioning that these dissociation energies build on the assumption that vibrational scaling factors perform equally well over the full intra- and intermolecular frequency range, despite the highly anharmonic nature of most intermolecular vibrational modes, in particular, in complexes such as $O_3(H_2O)$ or $(H_2O)_2$.[58–63] For instance, application of a single scaling factor [$\lambda_{CCSD(T)/aVDZ}$ = 0.971] for the water dimer $(H_2O)_2$ yields intramolecular frequencies with very small deviations in E_{ZPE} relative to experiment, i.e., the intramolecular E_{ZPE}(scaled) deviates from the measured value of E_{ZPE}(exp.) by no more than 0.1 kcal/mol. The very same scaling factor, however, gives rise to a large deviation in the intermolecular contribution to the zero-point energy. Specifically, the difference between values of E_{ZPE}(scaled) and the true E_{ZPE}(exp.) increases to around 0.4 kcal/mol if a single scaling factor is applied to both intra- and intermolecular modes (see Table 2S, supplementary material).

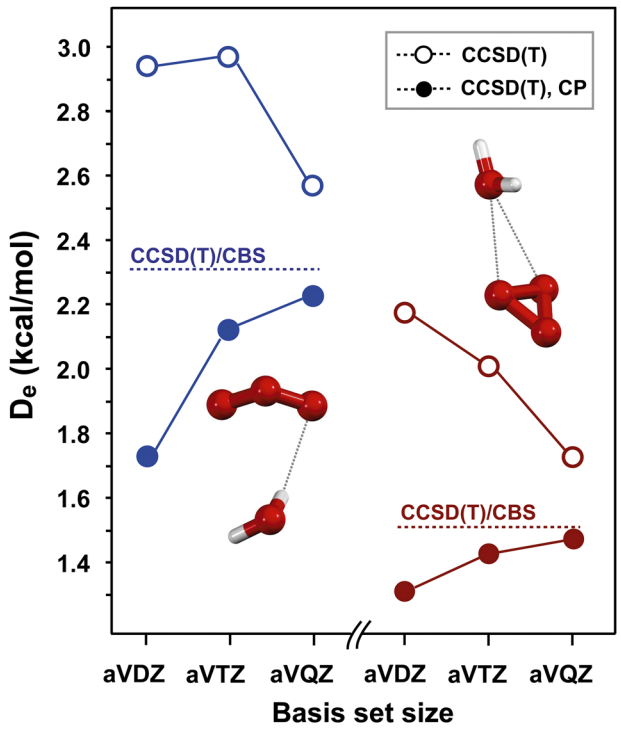

FIG. 3. CCSD(T)/aV*n*Z (*n* = D, T, Q) and complete basis set limit dissociation energies D_e (in kcal/mol) for $O_3(H_2O)$.

Also listed in Table III are anharmonic frequencies for the $O_3(H_2O)$ complex IA, and these have been calculated at the CCSD(T)/aV*n*Z (*n* = D, T) level of theory using the procedure outlined in Eq. (3). There are two experimental measurements of the vibrational frequencies in $O_3(H_2O)$, with a particular focus on the bending and stretching transitions in water and ozone across the frequency range 700 cm^{-1}–3700 cm^{-1}.[16,18] To the best of our knowledge, there are no IR spectroscopic measurements for $O_3(H_2O)$ in the intermolecular frequency range below 700 cm^{-1}. Calculated anharmonic CCSD(T)/aVDZ O_3 bending, asymmetric, and symmetric stretching vibrations in C_{2v} $O_3(H_2O)$ are ν_2 = 690 cm^{-1}, ν_3 = 890 cm^{-1}, and ν_1 = 1078 cm^{-1} (see Table III), and these deviate from experiment by −13 cm^{-1}, −155 cm^{-1}, and −32 cm^{-1}, respectively. Basis set expansion to aVTZ, however, gives rise to a significant improvement in the vibrational band positions, with smaller deviations at 9 cm^{-1}, −20 cm^{-1}, and 27 cm^{-1} for ν_2, ν_3, and ν_1, respectively. Table III also shows that the vibrational bands ν_2, ν_3, and ν_1 for ozone in $O_3(H_2O)$ are all blue-shifted relative to the O_3 monomer by around 6 cm^{-1}, 21 cm^{-1}, and 18 cm^{-1}, which is consistent with experimentally determined blue-shifts of 3 cm^{-1}–7 cm^{-1} for the bending and stretching transitions observed in $O_3(H_2O)$.[18] If we apply Eq. (7) together with our anharmonic CCSD(T)/aVTZ ν_i estimates for O_3, H_2O, and $O_3(H_2O)$ isomer IA, we arrive at $ZPE_F(O_3)$ = 4.10 kcal/mol, $ZPE_F(H_2O)$ = 12.85 kcal/mol, and $ZPE_F(O_3–H_2O)$ = 17.44 kcal/mol and a value of ΔZPE_F = 0.49 kcal/mol. Application of this ΔZPE_F value with our CCSD(T)/CBS dissociation energy value of D_e = 2.31 kcal/mol for $O_3(H_2O)$ IA provides a best estimate anharmonic CCSD(T)/aVTZ value for D_o = 2.31 − [17.44 − 12.85 − 4.10] = 1.82 kcal/mol.

TABLE III. CCSD(T)/aV*n*Z scaled-harmonic (ω, cm^{-1}), anharmonic (ν, cm^{-1}, intensities in km/mol), experimental frequencies ($\nu_{exp.}$), and anharmonic ZPEs (kcal/mol) for C_{2v} $O_3(H_2O)$ complex IA.

	ω_i		ν_i			$\nu_i - \nu_{exp.}$	
Assignment	aVDZ	aVTZ	aVDZ	aVTZ[a]	$\nu_{exp.}$	aVDZ	aVTZ
asym. O–H stretch (ν_3)	3784 (60)	3789 (63)	3697 (46)	3734	3727[b]	−30	7
sym. O–H stretch (ν_1)	3670 (6)	3690 (7)	3592 (4)	3644	3633[b]	−41	11
H–O–H bend (ν_2)	1590 (48)	1580 (55)	1595 (46)	1596	1598[c]	−3	−2
sym. O–O stretch (ν_1)	1087 (1)	1122 (1)	1078 (3)	1137	1110[c]	−32	27
asym. O–O stretch (ν_3)	945 (122)	1028 (130)	890 (99)	1025	1045[c]	−155	−20
O–O–O bend (ν_2)	689 (3)	700 (3)	690 (3)	712	703[c]	−13	9
Bound O–H wag	313 (126)	280 (129)	173 (56)	123			
Free O–H wag	135 (89)	142 (54)	39 (49)	78			
O_3 rock	140 (7)	133 (30)	92 (52)	41			
H_2O rock	101 (54)	94 (41)	68 (38)	39			
O_3 wag	85 (28)	72 (16)	61 (32)	41			
Inter. O_w-O_c stretch	72 (22)	67 (72)	37 (30)	33			
ZPE	18.03	18.15	17.17	17.44			
D_o	1.11[d]	1.20[d]	1.63[d]	1.82[d]			

[a]Calculated by Eq. (1).
[b]Reference 16 (Ar-matrix).
[c]Reference 18 (Ne-matrix).
[d]Calculated with CCSD(T)/CBS D_e.

C. D_{3h} $O_3(H_2O)$

We identified three $O_3(H_2O)$ isomers with D_{3h} ozone, and their structures are presented together with CCSD(T) relative energies and charges in Fig. 4. The lowest energy $O_3(H_2O)$ complex IS is a structure in which H_2O attaches to the ozone ring via two $O\cdots O_w$ contacts at 2.852 Å and 2.879 Å. A second minimum IT is a top-on configuration, in which one H atom of H_2O hydrogen-bonds with an ozone O atom, with the second hydrogen pointing toward the O_3 ring; a third $O_3(H_2O)$ minima IV at 0.42 kcal/mol maintains a single hydrogen-bond and bifurcated $O_c\cdots O_w$ contact. The energetic ranking at the CCSD(T)/CBS level of theory for isomers IS, IT, and IV is 0.0 kcal/mol, 0.2 kcal/mol, and 0.4 kcal/mol. In the case of isomer IS, there is only a small (almost null) charge-transfer between water and ozone; however, there is a noticeable intra-ring charge reorganization in this complex. For example, the two ozone O atoms proximal to H_2O sum up to a positive value of 0.04*e*, whereas the more distal O atom is reduced to −0.03*e*. The situation is different for isomers IT and IV, and unlike in IS, charge is transferred between O_3 and H_2O and reorganized across the ozone ring, i.e., the total H_2O to O_3 charge transfer in IT and IV is 0.05*e* and 0.06*e*, respectively, and thus, moderately larger than in the all open C_{2v} $O_3(H_2O)$ complexes.

The CP-uncorrected CCSD(T) dissociation energies D_e for complex IS are 2.17 kcal/mol (aVDZ), 2.02 kcal/mol (aVTZ), and 1.73 kcal/mol (aVQZ) and converge to 1.53 kcal/mol at the CBS limit (see Table IV); the CCSD(T)/CBS limit dissociation energies D_e for complexes IT and IV are 1.33 kcal/mol and 1.12 kcal/mol respectively. For isomer IS, the CP-corrected CCSD(T)/CBS dissociation energy is 1.51 kcal/mol, which aligns closely with the CP-uncorrected CCSD(T)/CBS value D_e = 1.53 kcal/mol. The CP-corrected values of D_e for IT and IV are 1.51 kcal/mol and 1.30 kcal/mol, respectively; as noted in the case of the open $O_3(H_2O)$ dimer complexes (i.e., IB, IC, ID), there are moderate differences between uncorrected and CP-corrected CCSD(T)/CBS dissociation energies, and in the case of D_{3h} $O_3(H_2O)$, these differences are on the order of 0.1 kcal/mol–0.2 kcal/mol.

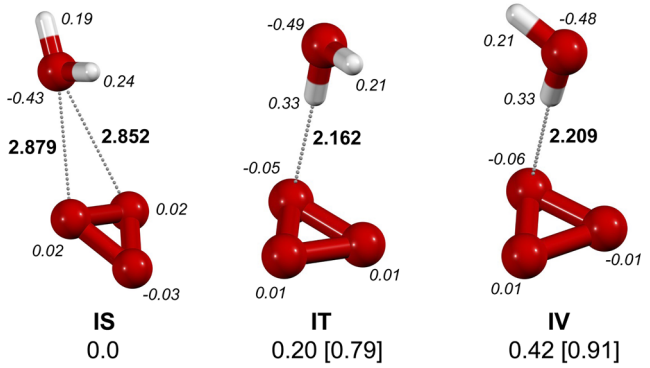

FIG. 4. CCSD(T)/aVTZ equilibrium structures (distances in Å), Mulliken charges (italicized), and CCSD(T)/CBS relative energies, without and with ZPE corrections (square brackets) in kcal/mol for $O_3(H_2O)$ complexes with cyclic ozone. IS–IV: non-planar.

TABLE IV. CCSD(T)/aV*n*Z dissociation energies (D_e) and scaled-harmonic dissociation energies (D_o) for D_{3h} $O_3(H_2O)$.

Isomer	Basis set	Energy (E_h)	D_e (kcal/mol)[a]	D_o (kcal/mol)[a]
IS	aVDZ	−301.203 167	2.17 [1.31]	1.40 [0.54]
	aVTZ	−301.509 722	2.02 [1.43]	1.42 [0.83]
	aVQZ[b]	−301.653 331	1.73 [1.48]	. . .
	CBS[D,T,Q][c]	−301.739 830	1.53 [1.51]	. . .
	CBS[T,Q][d]	−301.758 127	1.51 [1.52]	. . .
IT	aVDZ	−301.204 502	3.01 [1.26]	1.98 [0.24]
	aVTZ	−301.510 925	2.77 [1.37]	1.59 [0.18]
	aVQZ[b]	−301.653 621	1.91 [1.45]	. . .
	CBS[D,T,Q][c]	−301.739 507	1.33 [1.51]	. . .
	CBS[T,Q][d]	−301.757 751	1.28 [1.52]	. . .
IV	aVDZ	−301.204 454	2.98 [1.05]	1.87 [−0.05]
	aVTZ	−301.510 616	2.58 [1.15]	1.49 [0.06]
	aVQZ[b]	−301.653 289	1.70 [1.24]	. . .
	CBS[D,T,Q][c]	−301.739 169	1.12 [1.30]	. . .
	CBS[T,Q][d]	−301.757 402	1.06 [1.30]	. . .

[a]CP-corrected D_e and D_o in square brackets.
[b]SPC on aVTZ geometry.
[c]Calculated by fitting E_h values to Eq. (3).
[d]Calculated by fitting E_h values to Eq. (4).

The ZPE-corrected dissociation energies D_o are listed in Table IV. CCSD(T)/aVTZ values of D_o for complexes IS, IT, and IV are 1.42 kcal/mol, 1.59 kcal/mol, and 1.49 kcal/mol, and the corresponding CP-corrected D_o values are 0.83 kcal/mol, 0.18 kcal/mol, and 0.06 kcal/mol, respectively. We also calculated anharmonic CCSD(T)/aVTZ vibrational frequencies and dissociation energies D_o for the $O_3(H_2O)$ ring complexes IS and IT (see the supplementary material, Table 3S). As noted above, attachment of a single water molecule onto cyclic ozone results in a symmetry breaking from D_{3h} to lower C_s symmetry and splits the doubly degenerate bending mode ν_2 into two bands at 786 cm^{-1} and 803 cm^{-1}. Despite being only on the order of ~20 cm^{-1}, this spectral feature would provide a reliable diagnostic for the identification of cyclic ozone following complexation with water or a comparable solvent molecule. For comparison, symmetry breaking in the $O_3(H_2O)$ complex IT does not result in any noticeable splitting of the ν_2 band and, instead, shifts ν_2 from 797 cm^{-1} to 794 cm^{-1}, whereas the ν_3 band remains unchanged at 797 cm^{-1}. Combining CCSD(T)/CBS values of D_e with our anharmonic vibrational frequencies for the dimer complexes IS and IT yields CCSD(T)/aVTZ D_o values of 0.99 kcal/mol and 0.86 kcal/mol, respectively. These D_o estimates for D_{3h} $O_3(H_2O)$ complexes are only moderately smaller (by ~0.9 kcal/mol) compared against the CCSD(T) dissociation energy D_o = 1.82 kcal/mol of the lowest energy C_{2v} dimer IA.

D. C_{2v} $O_3(H_2O)_2$

Structures, relative energies, and charges for all five C_{2v} $O_3(H_2O)_2$ complexes IIA–IIE are presented in Fig. 5, and respective CCSD(T)/aVTZ dissociation energies are listed in Table V. For the

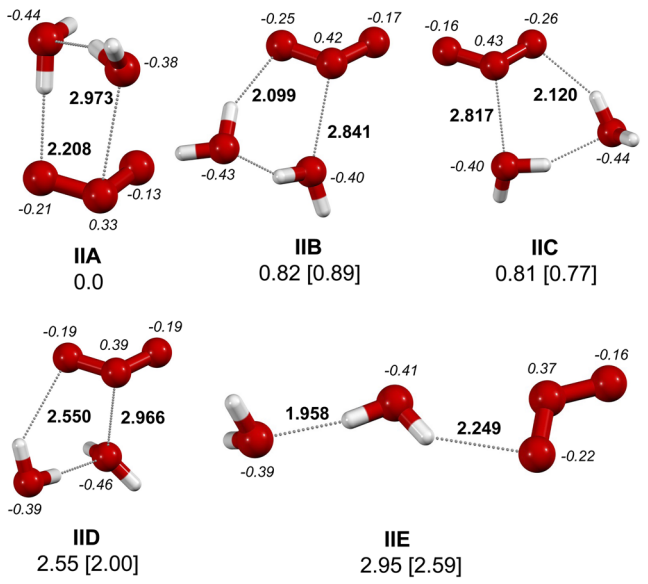

FIG. 5. CCSD(T)/aVDZ equilibrium structures (distances in Å), Mulliken charges (italicized), and CCSD(T)/aVTZ relative energies, without and with ZPE corrections (square brackets) in kcal/mol for C_{2v} $O_3(H_2O)_2$. IIA–IIE: non-planar.

global minimum $O_3(H_2O)_2$ complex IIA, the CCSD(T)/aVDZ intermolecular distance $r[O_c\cdots O_w]$ between ozone and water is 2.973 Å. Figure 5 also presents the results from a Mulliken population analysis for all O atoms, with hydrogen charges omitted for clarity. The O atom charges for the ozone and water molecules in the $O_3(H_2O)_2$ complex IIA reveal that the attachment of a second water molecule to the $O_3(H_2O)$ complex IA leads to a minor charge transfer (~0.01*e*) from water to ozone. There is, however, a significant charge redistribution across the ozone and water molecules in all $O_3(H_2O)_2$ complexes. Specifically, charge redistribution in the $O_3(H_2O)_2$ complex IIA leads to partial charges of −0.13*e* (O_t), −0.21*e* (O_t), and 0.33*e* (O_c) and O_w charges of −0.44*e* and −0.38*e*. These results are in good agreement with the findings from the B3LYP calculation for the same $O_3(H_2O)_2$ complex,[21] which yielded charges of −0.24*e*, −0.10*e*, and 0.33*e* for the ozone O_t and O_c sites, respectively, and −0.57*e* and −0.56*e* on the water O atoms. Consistent with our CCSD(T) charge calculations, two types of intermolecular interactions contribute toward the overall stability of $O_3(H_2O)_2$: (i) Coulombic $O_c\cdots O_w$ interactions between the positively charged (0.33*e*) ozone O_c and negatively charged (−0.38*e*) water O_w sites, with binding energies of ~2.7 kcal/mol, (ii) intermolecular $O_t\cdots H_w$ hydrogen-bonds (2.99 kcal/mol) bridging ozone and water, and (iii) relatively strong (5 kcal/mol) $O_w\cdots H_w$ hydrogen-bonds between water molecules that complete the three-member ring structures in isomers IIA–IID.

A survey of all possible $O_3(H_2O)_2$ structures shows that the ring-like complex IIA is the global minimum at the CCSD(T)/aVDZ level of theory, with IIB and IIC 0.8 kcal/mol and 0.9 kcal/mol higher in energy than IIA, respectively. One additional ring-like structure IID (2.5 kcal/mol) and a linear geometry IIE (2.8 kcal/mol), in which O_3 is bound via a terminal O_t position to a water dimer, are also local minima on the potential energy surface. Basis set expansion from aVDZ to aVTZ leads to a reordering of the CCSD(T) energies to 0.8 kcal/mol (IIB), 0.8 kcal/mol (IIC), 2.6 kcal/mol (IID), and 3.0 kcal/mol (IIE), respectively. Table V also lists the CCSD(T)/aVTZ level water dimer dissociation energies D_e for the reaction $O_3(H_2O)_2 = O_3 + (H_2O)_2$, and these are 5.7 kcal/mol (IIA), 4.9 kcal/mol (IIB), 4.9 kcal/mol (IIC), 3.1 kcal/mol (IID), and 2.7 kcal/mol (IIE), respectively; these values of D_e are only moderately larger (by 0.6 kcal/mol–1.1 kcal/mol) than the previously reported CCSD(T)/CBS D_e values for the dissociation of $O_3(H_2O)_2$ to ozone and an intact water dimer complex.[9,26]

We have also undertaken CCSD(T)/aVDZ anharmonic frequency calculations, with a focus on the global minimum IIA, in order to provide accurate values of the vibrational frequencies for structure IIA and their assignments (see Table VI). It is worth noting that CCSD(T) anharmonic frequency calculations for these systems are computationally very demanding, and thus, such frequencies are only reported for structure IIA. The $O_3(H_2O)_2$ complex IIA was optimized at the CCSD(T)/aVDZ level, and the corresponding anharmonic values for the C_{2v} O_3 symmetric (ν_1), asymmetric stretching (ν_3), and bending (ν_2) frequencies are 1070 cm^{-1}, 905 cm^{-1}, and 694 cm^{-1}, respectively. By comparison, ozone bending and stretching frequencies in $O_3(H_2O)_2$ IIA obtained from scaled harmonic CCSD(T)/aVDZ calculations are ν_1 = 1094 cm^{-1}, ν_3 = 953 cm^{-1}, and ν_2 = 696 cm^{-1}, which are, with the exception of the asymmetric stretch ν_3, in good agreement with the results from anharmonic calculations (see Table VI). The most striking feature, however, is the systematic shift in the vibrational bands of ozone with increasing water numbers and therefore its sensitivity to the ozone hydration environment. For instance, values of ν_1, ν_3, and ν_2 for $O_3(H_2O)_2$ are all shifted to the blue (relative to O_3) by 14 cm^{-1}, 17 cm^{-1}, and 9 cm^{-1}, respectively, because the motion of the O_3 molecule is hindered by water molecules hydrogen-bonding to the ozone O_t and O_c atom sites.

TABLE V. CCSD(T)/aV*n*Z dissociation energies (D_e) and scaled-harmonic dissociation energies (D_o) for C_{2v} $O_3(H_2O)_2$.

Isomer	Basis set	Energy (E_h)	D_e (kcal/mol)[a]	D_o (kcal/mol)[a]
IIA	aVDZ	−377.545 099	5.48 [3.62]	4.20 [2.34]
	aVTZ[b]	−377.929 183	5.68 [4.15]	. . .
IIB	aVDZ	−377.543 782	4.65 [2.90]	3.30 [1.54]
	aVTZ[b]	−377.927 875	4.86 [3.36]	. . .
IIC	aVDZ	−377.543 645	4.56 [2.97]	3.32 [1.73]
	aVTZ[b]	−377.927 898	4.87 [3.44]	. . .
IID	aVDZ	−377.541 143	2.99 [1.53]	2.26 [0.80]
	aVTZ[b]	−377.925 125	3.13 [2.02]	. . .
IIE	aVDZ	−377.540 682	2.71 [1.54]	1.79 [0.63]
	aVTZ[b]	−377.924 474	2.72 [1.75]	. . .

[a] $O_3(H_2O)_2 = O_3 + (H_2O)_2$; CP-corrected D_e and D_o in square brackets.
[b] SPC on aVDZ geometry.

TABLE VI. CCSD(T)/aVDZ scaled-harmonic (ω_i, cm^{-1}), anharmonic (ν_i, cm^{-1}, intensities in km/mol), and anharmonic ZPEs (kcal/mol) for C_{2v} $O_3(H_2O)_2$ IIA.

Assignment	ω_i	ν_i
ac. asym. O–H stretch (ν_3)	3767 (124)	3682 (57)
do. asym. O–H stretch (ν_3)	3764 (64)	3675 (12)
ac. sym. O–H stretch (ν_1)	3650 (69)	3579 (33)
do. sym. O–H stretch (ν_1)	3574 (226)	3520 (137)
do. H–O–H bend (ν_2)	1610 (38)	1612 (23)
ac. H–O–H bend (ν_2)	1590 (60)	1598 (55)
sym. O–O stretch (ν_1)	1094 (3)	1070 (7)
asym. O–O stretch (ν_3)	953 (116)	905 (91)
O–O–O bend (ν_2)	696 (3)	694 (13)
	650 (74)	536 (—)
	458 (87)	397 (68)
	274 (161)	255 (—)
	192 (57)	161 (26)
	179 (36)	166 (193)
	177 (74)	79 (66)
	139 (19)	126 (76)
	113 (79)	81 (11)
	105 (8)	82 (41)
	85 (13)	79 (4)
	82 (2)	78 (11)
	45 (0)	38 (1)
ZPE	33.16	32.04
D_o	2.87[a]	3.08[b]

[a]CCSD(T)/aVTZ D_e with CCSD(T)/aVDZ ΔZPE_H.
[b]CCSD(T)/aVTZ D_e with CCSD(T)/aVDZ ΔZPE_F.

Table VI lists the CCSD(T)/aVDZ level of theory ZPE_H and ZPE_F values and corresponding dissociation energies D_o for the $O_3(H_2O)_2$ isomer IIA. The dissociation energy D_o, according to $O_3(H_2O)_2 = O_3 + (H_2O)_2$, has been determined previously using QCISD/aVTZ level calculations and is 3.35 kcal/mol.[9] Our anharmonic ΔZPE_F for the dissociation of structure IIA is 1.07 kcal/mol and, in combination with a CP-corrected CCSD(T)/aVDZ D_e value of 3.62 kcal/mol, leads to a slightly smaller anharmonic dissociation energy of $D_o = D_e - \Delta ZPE_F = 3.62 - 1.07 = 2.34$ kcal/mol; the corresponding anharmonic CCSD(T)/aVTZ dissociation energy D_o using $\Delta ZPE_F = 1.07$ kcal/mol and $D_e = 4.15$ kcal/mol is 3.08 kcal/mol. We anticipate that a part of this ~0.3 kcal/mol discrepancy in D_o between our CCSD(T)/aVTZ and QCISD/aVTZ results reported by Anglada *et al.*[9] can be attributed to the neglect of anharmonicity in the work of these authors and their use of a general scaling factor (0.965) for all vibrational modes in $O_3(H_2O)_2$. Finally, Yadav *et al.*[21] reported a $O_3(H_2O)_2$ IIA dissociation energy of $D_o = 4.39$ kcal/mol using B3LYP/6-311+G(*d*,*p*) level calculations, which would not require basis set superposition error (BSSE) correction but would likely suffer from the neglect of anharmonicity. The results of our current calculations for $O_3(H_2O)_2$ IIA suggest that a 1.07 kcal/mol for ΔZPE_F and CCSD(T)/aVTZ value of $D_e = 4.15$ kcal/mol would lead to a best estimate anharmonic CCSD(T) level dissociation energy $D_o = 3.08$ kcal/mol.

TABLE VII. CCSD(T)/aV*n*Z dissociation energies (D_e) and scaled-harmonic dissociation energies (D_o) for D_{3h} $O_3(H_2O)_2$.

Isomer	Basis set	Energy (E_h)	D_e (kcal/mol)[a]	D_o (kcal/mol)[a]
IIV	aVDZ	−377.492 307	4.95 [2.67]	3.72 [1.44]
	aVTZ[b]	−377.879 196	4.49 [2.64]	. . .
IIT	aVDZ	−377.489 268	3.04 [1.15]	2.18 [0.29]
	aVTZ[b]	−377.876 666	2.90 [1.37]	. . .
IIS	aVDZ	−377.488 212	2.38 [1.60]	1.81 [1.04]
	aVTZ[b]	−377.875 875	2.40 [1.71]	. . .
IIM	aVDZ	−377.484 305	2.29 [0.96]	1.17 [−0.16]
	aVTZ[b]	−377.870 501	2.03 [0.80]	. . .

[a]$O_3(H_2O)_2 = O_3 + (H_2O)_2$ for IIT, IIS, IIV; $O_3(H_2O)_2 = O_3(H_2O) + H_2O$ for IIM; CP-corrected D_e and D_o in square brackets.
[b]SPC on aVDZ geometry.

E. D_{3h} $O_3(H_2O)_2$

Table VII lists $O_3(H_2O)_2$ energies (E_h) and dissociation energies for four isomers with D_{3h} ozone, and these structures are also presented in Fig. 6 together with their charges. Complex IIV is the global minimum structure at all levels of theory, i.e., CCSD(T)/aVDZ and CCSD(T)/aVTZ, and is separated from the local minima IIT, IIS, and IIM by 1.9 kcal/mol, 2.6 kcal/mol, and 5.0 kcal/mol, respectively. Basis set expansion from aVDZ to aVTZ does not change the energetic ordering; however, the first three complexes are energetically more closely spaced at 1.6 kcal/mol (IIT) and 2.1 kcal/mol (IIS), with one less stable structure IIM at 5.5 kcal/mol.

Dissociation energies D_e (with and without CP-correction) for complexes IIV, IIT, and IIS according to $O_3(H_2O)_2 = O_3 + (H_2O)_2$ are listed in Table VII together with ZPE-corrected values of D_o. The CCSD(T)/aVDZ values of D_e are 4.95 kcal/mol (IIV), 3.04 kcal/mol (IIT), 2.38 kcal/mol (IIS), and 2.29 kcal/mol (IIM) and generally

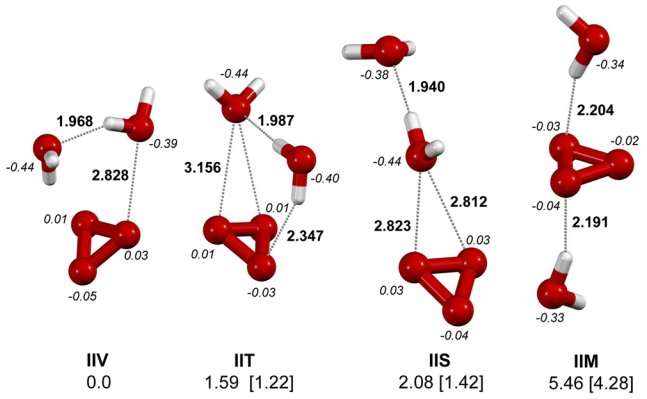

FIG. 6. CCSD(T)/aVDZ equilibrium structures (distances in Å), Mulliken charges (italicized), and CCSD(T)/aVTZ relative energies, without and with ZPE corrections (square brackets) in kcal/mol for D_{3h} $O_3(H_2O)_2$. IIV–IIM: non-planar.

shift to smaller values, 4.49 kcal/mol (IIV), 2.90 kcal/mol (IIT), 2.40 kcal/mol (IIS), and 2.03 kcal/mol (IIM), as the basis set increases from aVDZ to aVTZ. Table VII also presents results of harmonic frequency calculations for all four isomers using a scaling factor of $\lambda = 0.971$, and these are given as CP-corrected dissociation energies D_o (listed in brackets). At the CCSD(T)/aVDZ level of theory, the range of D_o values was found to be 1.44 kcal/mol (IIV), 0.29 kcal/mol (IIT), 1.04 kcal/mol (IIS), and −0.16 kcal/mol (IIM). It is noteworthy that with CP-correction, the values of D_o decrease by up to 1 kcal/mol–2 kcal/mol, making the binding generally weaker. For example, in the case of the $O_3(H_2O)_2$ complex IIM, CP-corrections shift the dissociation energies to negative values, and thus, in this case, the magnitude of the counterpoise correction is larger than the binding energy itself.

Anharmonic CCSD(T)/aVDZ frequencies for the D_{3h} $O_3(H_2O)_2$ complex IIV have been calculated, and these results are listed in Table 4S together with their respective vibrational band assignments and anharmonic dissociation energy D_o. The symmetric stretching mode (ν_1) for cyclic O_3 in $O_3(H_2O)_2$ is predicted at 1032 cm^{-1}, and asymmetric stretching (ν_3) and bending (ν_2) modes are at 739 cm^{-1} and 758 cm^{-1}, respectively, and therefore red- (9 cm^{-1}) and blue-shifted (10 cm^{-1}) relative to the free ozone ring (748 cm^{-1}). Combining our anharmonic zero-point energy difference (ΔZPE_F = 0.96 kcal/mol) for the dissociation of the D_{3h} $O_3(H_2O)_2$ complex IIV with a CCSD(T)/aVDZ D_e value of 2.67 kcal/mol provides an anharmonic dissociation energy $D_o = D_e - \Delta ZPE_F = 2.67 - 0.96 = 1.71$ kcal/mol, which is around 0.2 kcal/mol larger than the scaled-harmonic CCSD(T)/aVDZ dissociation energy D_o of 1.44 kcal/mol. Increasing the basis set from aVDZ to aVTZ decreases the dissociation energy D_o by around ~0.03 kcal/mol, and in this case, $D_o = D_e - \Delta ZPE_F = 2.64 - 0.96 = 1.68$ kcal/mol. In conclusion, given that anharmonic frequency calculations at the CCSD(T)/aVTZ level of theory are currently not feasible, we would recommend a value of 1.68 kcal/mol as the best estimate of D_o for D_{3h} $O_3(H_2O)_2$.

F. CPMD simulation

We have complemented our CCSD(T)/aV*n*Z study of $O_3(H_2O)_{1,2}$ with a set of exploratory CPMD calculations aimed at probing the solvation dynamics in C_{2v} $O_3(H_2O)$ and $O_3(H_2O)_2$ complexes, with a particular focus on temperature-induced changes in the configuration and stability of both species. Three simulation temperatures were chosen, 50 K, 100 K, and 150 K, in order to examine dynamic structures of $O_3(H_2O)$ and $O_3(H_2O)_2$ but also to provide some guidance on selecting suitable conditions in IR spectroscopic studies of this system. Our CPMD results are presented as distance $r[O_c\cdots O_w]$ vs time profiles and are shown in Fig. 7 up to 30 ps simulation time. First, it is worth to briefly comment on the predictive power of our CPMD simulation results. As a demonstration, we use $O_3(H_2O)$ and $(H_2O)_2$ as a test set and compare binding energies and structure parameters from CCSD(T) calculations against those obtained from BLYP CPMD simulations. The $O_3(H_2O)$ CCSD(T)/aVTZ dissociation energy is 1.82 kcal/mol and closely matches the BLYP CPMD level value of 1.79 kcal/mol. The dissociation energies at the CCSD(T)/aVDZ and BLYP CPMD level of theory for $(H_2O)_2$ are D_o = 3.59 kcal/mol and 3.02 kcal/mol, respectively, and are well within a target accuracy of ~1 kcal/mol. The structural output from CCSD(T) and CPMD calculations is also

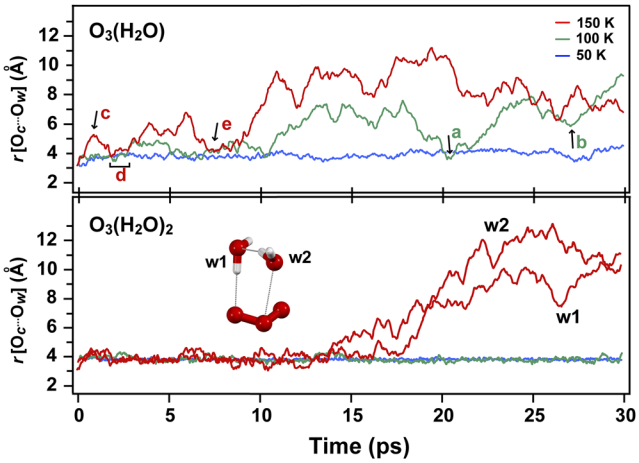

FIG. 7. CPMD time series of the interoxygen distance $r[O_c\cdots O_w]$ (Å) for C_{2v} $O_3(H_2O)_n$ (n = 1–2) at 50 K, 100 K, and 150 K.

in good agreement, with $O_w\cdots O_w$ distances in $(H_2O)_2$ at 3.245 Å (BLYP CPMD) and 2.920 Å with the CCSD(T)/aVDZ level of theory. Finally, BLYP CPMD is in fair agreement with the CCSD(T)/aVDZ results for the $O_c\cdots O_w$ separation distance in $O_3(H_2O)$ and comes within 0.402 Å of CCSD(T).

We will at first consider the solvation behavior of $O_3(H_2O)$ at 50 K, with the purpose of understanding how water binds to ozone under cryogenic conditions, but also as a reference point for higher-temperature CPMD simulations of $O_3(H_2O)$. As seen from Fig. 7, the $O_3(H_2O)$ configuration at 50 K (blue trace) remains intact throughout the full 30 ps simulation period. We observed minor fluctuations in the intermolecular distance $r[O_c\cdots O_w]$ between ozone and water, ranging from 3.1 Å to 4.5 Å, and these changes are due to the H_2O molecule performing a full rotation around O_3. These results also demonstrate that water attaches via a $O_t\cdots H_w$ type hydrogen-bond to ozone, and this linkage is maintained throughout most of the 30 ps CPMD simulation; this configuration is also consistent with the structure recognized from CCSD(T)/aVTZ geometry optimizations reported in Sec. III B.

The solvation of ozone was further examined at higher temperatures, and Fig. 7 shows the water solvation dynamics in $O_3(H_2O)$ over a 30 ps time period as green (100 K) and red (150 K) traces for the intermolecular distance $r[O_c\cdots O_w]$, respectively. A temperature increase from 50 K to 100 K results in the detachment of H_2O from O_3: for instance, starting at around 10 ps, water begins to dissociate from O_3, and the values of $r[O_c\cdots O_w]$ increases steadily as a function of time from 3.8 Å at 10.5 ps to 9.2 Å at 30 ps, with the exception of a brief period from 18 ps to 20 ps, where values of $r[O_c\cdots O_w]$ reduce from 7.5 Å to 3.6 Å due to the formation of a transient $O_t\cdots O_w$ contact (point a in Fig. 7). The results from CPMD simulations of $O_3(H_2O)$ at 100 K can be subdivided down into three distinct phases: first, starting at 9 ps, the $O_t\cdots H_w$ hydrogen-bond in $O_3(H_2O)$ is ruptured and reaches a maximum separation of ~8 Å; second, beginning at 17 ps, H_2O and O_3 reassociate and form a transient complex with a $r[O_c\cdots O_w]$ range of 3.5 Å–4.0 Å and a life-time of ~1.5 ps; finally, the $O_t\cdots O_w$ contact in $O_3(H_2O)$ is broken, and

starting at ~27 ps (point b, Fig. 7), H_2O irreversibly dissociates from O_3 reaching a maximum separation $r[O_c\cdots O_w]$ of 9.0 Å toward the final stage of the simulation at 30 ps.

The ozone solvation dynamics at 150 K are distinctly different from the CPMD results at 50 K and 100 K. Starting at ~0.5 ps, H_2O dissociates from O_3 (point c, Fig. 7) and rebinds to O_3 at ~1.5 ps temporarily preserving the intact $O_3(H_2O)$ structure; the life-time of this transient structure is around 1 ps–1.5 ps (point d, Fig. 7), with a time-averaged $r[O_c\cdots O_w]$ distance of 3.7 Å–4.1 Å. Starting at ~8 ps, the $O_t\cdots H_w$ hydrogen-bond in $O_3(H_2O)$ is irreversibly severed (point e, Fig. 7), with O_3 and H_2O continuously separating for the remaining 22 ps duration of the simulation. These results demonstrate that the $O_t\cdots H_w$ hydrogen-bond in $O_3(H_2O)$ is thermally labile at 150 K and would certainly rupture at lower temperatures, i.e., 100 K.

In order to shed light on the solvation dynamics of ozone, we also include the results from CPMD simulations of the trimer complex $O_3(H_2O)_2$ in the range 50 K–150 K and compare these results with those made for the dimer complex $O_3(H_2O)$. As seen from Fig. 7, the structure of $O_3(H_2O)_2$ at 50 K remains fully preserved over the entire 30 ps simulation period, following rearrangement (after ~1 ps) from a structure with an extended $O_c\cdots O_w$ (2.97 Å) to a shorter $O_t\cdots O_w$ contact (2.71 Å). The solvation dynamics of $O_3(H_2O)_2$ was further examined at 100 K and 150 K, and these results differ significantly from those obtained at 50 K. The most puzzling feature in the 100 K simulation of $O_3(H_2O)_2$ is that the trimer structure remains intact throughout the full 30 ps trajectory, whereas the $O_3(H_2O)$ dimer undergoes complete dissociation at the same temperature. A possible explanation for this enhanced stability of $O_3(H_2O)_2$ vs $O_3(H_2O)$ is that the former is a ring-shaped complex stabilized by two intermolecular $O_c\cdots O_w$ and $O_t\cdots H_w$ bonds, each at 0.91 kcal/mol and 1.88 kcal/mol, respectively, and a relatively strong (3.67 kcal/mol) $O_w\cdots H_w$ water bridge. These results, in particular, those at 100 K, demonstrate that the $O_3(H_2O)_2$ complex is considerably more stable against dissociation than $O_3(H_2O)$, in other words, the solvation of O_3 with second H_2O molecule has a stabilizing effect on the ozone–water system. The situation is quite different at 150 K, in that both water molecules, beginning at around 13 ps, dissociate from $O_3(H_2O)_2$ and are fully separated at distances >10 Å toward the final stage of the 30 ps simulation. In summary, our CPMD simulations demonstrate that the $O_3(H_2O)$ complex remains largely intact at 50 K, whereas at higher temperatures, i.e., 100 K–150 K, the water molecule begins to move away from $O_3(H_2O)$, resulting in a rapid and complete dissociation of this complex at 150 K. Finally, a particular point of interest is the stabilization effect induced by the second H_2O molecule in $O_3(H_2O)_2$, which is rooted in the strong Coulombic and hydrogen-bonding interactions that ultimately prevent it from dissociating at 50 K–100 K and thus, in principle, would render this complex spectroscopically observable.

IV. CONCLUSIONS

We have undertaken anharmonic CCSD(T)/CBS level calculations in order to determine equilibrium structures, energies, and anharmonic vibrational spectra of the ozone–water complexes $O_3(H_2O)_n$ (n = 1, 2). The most accurate inter-oxygen distance $O_c\cdots O_w$ in the global minimum of $O_3(H_2O)$ is 3.097 Å at the CCSD(T)/aVTZ level of theory, and this value compares favorably with an experimental estimate of 2.957 Å.[20] Our best estimate CCSD(T)/CBS values of D_e and D_o [with CCSD(T)/aVTZ ΔZPE_F corrections] for $O_3(H_2O)$ are 2.31 kcal/mol and 1.82 kcal/mol, respectively. Anharmonic CCSD(T)/aVTZ calculations predict ozone stretching and bending frequencies for $O_3(H_2O)$ at 1137 (ν_1) cm^{-1}, 1025 (ν_3) cm^{-1}, and 712 (ν_2) cm^{-1}, and these are in good agreement with the measured values reported by Tsuge *et al.*[18] The present work also considered $O_3(H_2O)$ complexes containing cyclic ozone, and CCSD(T)/CBS calculations predict a D_{3h} $O_3(H_2O)$ dissociation energy of D_e = 1.51 kcal/mol and a corresponding anharmonic CCSD(T) value of D_o = 0.99 kcal/mol, the latter being the most accurate determination for the cyclic $O_3(H_2O)$ complex to date.

We have also calculated the equilibrium structures, energies, and anharmonic vibrational spectra of the C_{2v} and D_{3h} $O_3(H_2O)_2$ trimer complexes. The best estimate CCSD(T)/aVTZ values of D_e and anharmonic D_o for C_{2v} $O_3(H_2O)_2$ are 4.15 kcal/mol and 3.08 kcal/mol, with two equidistant interoxygen contacts $O_c\cdots O_w$ and $O_t\cdots O_w$ at 2.973 Å and 3.050 Å, respectively. For D_{3h} $O_3(H_2O)_2$, we arrive at CCSD(T)/aVTZ estimates of D_e = 2.64 kcal/mol and D_o = 1.68 kcal/mol.

We also report the results from CPMD simulations of the C_{2v} $O_3(H_2O)$ and $O_3(H_2O)_2$ complexes at temperatures from 50 K to 150 K. CPMD calculations of $O_3(H_2O)$ show that a singly coordinated $O_3(H_2O)$ complex with a short $O_c\cdots O_w$ contact (~3.8 Å) is the most favored configuration, and this structure is preserved up to the dissociation limit at T ~ 100 K. This situation changes fundamentally upon increasing the temperature to 150 K. At this temperature, the $O_3(H_2O)$ complex remains initially intact and bound via a single $O_t\cdots H_w$ hydrogen bond up to ~8 ps into the course of the simulation and then ultimately dissociates.

The results from CPMD simulations of the $O_3(H_2O)_2$ trimer complex show a distinctly different behavior compared against those for the $O_3(H_2O)$ dimer: upon solvating $O_3(H_2O)$ with a second water molecule at 50 K and 100 K, we find that the $O_3(H_2O)_2$ complex remains largely intact over the entire 30 ps course of the simulation and undergoes full dissociation only at 150 K. At first glance, these results appear surprising that the $O_3(H_2O)_2$ complex remains intact up to 100 K, whereas $O_3(H_2O)$ undergoes full dissociation at the same temperature. These results can be best reconciled by reviewing the intermolecular interactions that contribute toward the overall stability of the $O_3(H_2O)$ vs $O_3(H_2O)_2$ complexes at 100 K. For $O_3(H_2O)$, the $O_t\cdots H_w$ hydrogen-bond energy is around 1.8 kcal/mol, whereas in the case of $O_3(H_2O)_2$, the average interaction energy due to hydrogen-bonding and $O_c\cdots O_w$ type interactions is slightly larger at 2.2 kcal/mol. In other words, the average binding energy in $O_3(H_2O)_2$ at 100 K is around 0.4 kcal/mol or 22% larger than in $O_3(H_2O)$. These results also imply that the enhanced stability of $O_3(H_2O)_2$ would give rise to a elevated trimer/dimer population ratio, thus making the trimer a spectroscopically detectable complex at cryogenic temperatures.

SUPPLEMENTARY MATERIAL

See the supplementary material for the vibrational frequencies of H_2O, $(H_2O)_2$, D_{3h} $O_3(H_2O)$, and $O_3(H_2O)_2$ and the

CCSD(T)/aVnZ level of theory Cartesian coordinates of the ozone–water complexes examined.

ACKNOWLEDGMENTS

This research was supported by the HK General Research Fund HKU (Grant Nos. 17330216 and 17307118). Computing time for this study was provided to W.C.H.H. and K.H.L. by the HKU High Performance Computing (Grant No. HPC2015) Center.

DATA AVAILABILITY

The data that support the findings of this study are available within the article and its supplementary material.

REFERENCES

[1]D. B. Kirk-Davidoff, E. J. Hintsa, J. G. Anderson, and D. W. Keith, Nature **402**, 399 (1999).
[2]D. S. King, D. G. Sauder, and M. P. Casassa, J. Chem. Phys. **100**, 4200 (1994).
[3]V. Vaida, G. J. Frost, L. A. Brown, R. Naaman, and Y. Hurwitz, Ber. Bunsengesellschaft Phys. Chem. **99**, 371 (1995).
[4]G. J. Frost and V. Vaida, J. Geophys. Res.: Atmos. **100**, 18803, https://doi.org/10.1029/95jd01940 (1995).
[5]P. T. Buckley and J. W. Birks, Atmos. Environ. **29**, 2409 (1995).
[6]J. Lelieveld, F. J. Dentener, W. Peters, and M. C. Krol, Atmos. Chem. Phys. **4**, 2337 (2004).
[7]A. Léger, M. Ollivier, K. Altwegg, and N. J. Woolf, Astron. Astrophys. **341**, 304 (1999).
[8]P. S. Monks, A. T. Archibald, A. Colette, O. Cooper, M. Coyle, R. Derwent, D. Fowler, C. Granier, K. S. Law, G. E. Mills, D. S. Stevenson, O. Tarasova, V. Thouret, E. von Schneidemesser, R. Sommariva, O. Wild, and M. L. Williams, Atmos. Chem. Phys. **15**, 8889 (2015).
[9]J. M. Anglada, G. J. Hoffman, L. V. Slipchenko, M. M. Costa, M. F. Ruiz-López, and J. S. Francisco, J. Phys. Chem. A **117**, 10381 (2013).
[10]B. E. Rocher-Casterline, L. C. Ch'ng, A. K. Mollner, and H. Reisler, J. Chem. Phys. **134**, 211101 (2011).
[11]K. M. Dreux and G. S. Tschumper, Comput. Theor. Chem. **1072**, 21 (2015).
[12]T. L. Ellington and G. S. Tschumper, Comput. Theor. Chem. **1021**, 109 (2013).
[13]M. Gussoni, M. Rui, and G. Zerbi, J. Mol. Struct. **447**, 163 (1998).
[14]T. N. Olney, N. M. Cann, G. Cooper, and C. E. Brion, Chem. Phys. **223**, 59 (1997).
[15]L. Nord, J. Mol. Struct. **96**, 37 (1983).
[16]L. Schriver, C. Barreau, and A. Schriver, Chem. Phys. **140**, 429 (1990).
[17]K. Jaeger, M. Wierzejewska-Hnat, and O. Schrems, Proc. SPIE **1575**, 331 (1992).
[18]M. Tsuge, K. Tsuji, A. Kawai, and K. Shibuya, J. Phys. Chem. A **111**, 3540 (2007).
[19]M. Tsuge, K. Tsuji, A. Kawai, and K. Shibuya, J. Phys. Chem. A **117**, 13105 (2013).
[20]J. Z. Gillies, C. W. Gillies, R. D. Suenram, F. J. Lovas, T. Schmidt, and D. Cremer, J. Mol. Spectrosc. **146**, 493 (1991).
[21]S. Yadav, S. Nawani, and N. Goel, J. Cluster Sci. **28**, 1693 (2017).
[22]I. I. Zakharov, O. I. Kolbasina, T. N. Semenyuk, N. F. Tyupalo, and G. M. Zhidomirov, J. Struct. Chem. **34**, 359 (1993).
[23]H. Tachikawa and S. Abe, Inorg. Chem. **42**, 2188 (2003).
[24]H. Tachikawa and S. Abe, Inorg. Chim. Acta **358**, 288 (2005).
[25]O. A. Loboda and V. V. Goncharuk, J. Water Chem. Technol. **31**, 213 (2009).
[26]P. Kumar and N. Sathyamurthy, Chem. Phys. **415**, 214 (2013).
[27]X. Wang, L. Liu, W. Fang, and X. Chen, Chem. Phys. Lett. **608**, 95 (2014).
[28]T. H. Dunning, Jr., J. Chem. Phys. **90**, 1007 (1989).
[29]J. F. Stanton, W. N. Lipscomb, D. H. Magers, and R. J. Bartlett, J. Chem. Phys. **90**, 1077 (1989).
[30]D. H. Magers, W. N. Lipscomb, R. J. Bartlett, and J. F. Stanton, J. Chem. Phys. **91**, 1945 (1989).
[31]K. A. Peterson, D. E. Woon, and T. H. Dunning, Jr., J. Chem. Phys. **100**, 7410 (1994).
[32]T. Helgaker, W. Klopper, H. Koch, and J. Noga, J. Chem. Phys. **106**, 9639 (1997).
[33]CFOUR, a quantum chemical program package written by J. F. Stanton, J. Gauss, L. Cheng, M. E. Harding, D. A. Matthews, P. G. Szalay with contributions from A. A. Auer, R. J. Bartlett, U. Benedikt, C. Berger, D. E. Bernholdt, Y. J. Bomble, O. Christiansen, F. Engel, R. Faber, M. Heckert, O. Heun, C. Huber, T.-C. Jagau, D. Jonsson, J. Jusélius, K. Klein, W. J. Lauderdale, F. Lipparini, T. Metzroth, L. A. Mück, D. P. O'Neill, D. R. Price, E. Prochnow, C. Puzzarini, K. Ruud, F. Schiffmann, W. Schwalbach, C. Simmons, S. Stopkowicz, A. Tajti, J. Vázquez, F. Wang, J. D. Watts and the integral packages MOLECULE (J. Almlöf and P. R. Taylor), PROPS (P. R. Taylor), ABACUS (T. Helgaker, H. J. Aa. Jensen, P. Jørgensen, and J. Olsen), and ECP routines by A. V. Mitin and C. van Wüllen. For the current version, see http://www.cfour.de.
[34]M. E. Harding, T. Metzroth, J. Gauss, and A. A. Auer, J. Chem. Theory Comput. **4**, 64 (2008).
[35].M. J. Frisch *et al.*, Gaussian 09, Revision D.01, Gaussian, Inc., Wallingford, CT, 2009.
[36].J. Hutter *et al.*, CPMD: An *Ab Initio* Electronic Structure and Molecular Dynamics Program, see http://www.cpmd.org.
[37]A. D. Becke, Phys. Rev. A **38**, 3098 (1988).
[38]C. Lee, W. Yang, and R. G. Parr, Phys. Rev. B **37**, 785 (1988).
[39]N. Troullier and J. L. Martins, Phys. Rev. B **43**, 1993 (1991).
[40]W. S. Benedict, N. Gailar, and E. K. Plyler, J. Chem. Phys. **24**, 1139 (1956).
[41]J. Ceponkus, P. Uvdal, and B. Nelander, J. Chem. Phys. **138**, 244305 (2013).
[42]V. G. Tyuterev, S. Tashkun, P. Jensen, A. Barbe, and T. Cours, J. Mol. Spectrosc. **198**, 57 (1999).
[43]P. Brosset, R. Dahoo, B. Gauthier-Roy, L. Abouaf-Marguin, and A. Lakhlifi, Chem. Phys. **172**, 315 (1993).
[44]J. D. Watts, J. F. Stanton, and R. J. Bartlett, Chem. Phys. Lett. **178**, 471 (1991).
[45]T. J. Lee and G. E. Scuseria, J. Chem. Phys. **93**, 489 (1990).
[46]A. Kalemos and A. Mavridis, J. Chem. Phys. **129**, 054312 (2008).
[47]D. Xie, H. Guo, and K. A. Peterson, J. Chem. Phys. **112**, 8378 (2000).
[48]F. Jensen, *Introduction to Computational Chemistry* (John Wiley & Sons, 2017).
[49]Z. W. Qu, H. Zhu, and R. Schinke, J. Chem. Phys. **123**, 204324 (2005).
[50]R. Siebert and R. Schinke, J. Chem. Phys. **119**, 3092 (2003).
[51]J. L. Chen and W. P. Hu, J. Am. Chem. Soc. **133**, 16045 (2011).
[52]E. Miliordos and S. Xantheas, J. Am. Chem. Soc. **136**, 2808 (2014).
[53]K. A. Peterson and T. H. Dunning, Jr., J. Chem. Phys. **102**, 2032 (1995).
[54]J. R. Alvarez-Idaboy and A. Dunning, Theor. Chem. Acc. **126**, 75 (2010).
[55]K. H. Lemke, J. Chem. Phys. **146**, 234301 (2017).
[56]S. K. Min, E. C. Lee, H. M. Lee, D. Y. Kim, D. Kim, and K. S. Kim, J. Comput. Chem. **29**, 1208 (2008).
[57]L. M. Azofra, I. Alkorta, and S. Scheiner, J. Chem. Phys. **140**, 244311 (2014).
[58]J. C. Howard, J. L. Gray, A. J. Hardwick, L. T. Nguyen, and G. S. Tschumper, J. Chem. Theory Comput. **10**, 5426 (2014).
[59]Z. S. Huang and R. E. Miller, J. Chem. Phys. **91**, 6613 (1989).
[60]U. Buck and F. Huisken, Chem. Rev. **100**, 3863 (2000).
[61]Y. Bouteiller and J. P. Perchard, Chem. Phys. **305**, 1 (2004).
[62]F. N. Keutsch, L. B. Braly, M. G. Brown, H. A. Harker, P. B. Petersen, C. Leforestier, and R. J. Saykally, J. Chem. Phys. **119**, 8927 (2003).
[63]L. B. Braly, K. Liu, M. G. Brown, F. N. Keutsch, R. S. Fellers, and R. J. Saykally, J. Chem. Phys. **112**, 10314 (2000).